



STRATOSPHERE

Pyrocumulonimbus affect average stratospheric aerosol composition

J. M. Katich^{1,2†}, E. C. Apel³, I. Bourgeois^{1,2}, C. A. Brock¹, T. P. Bu⁴, P. Campuzano-Jost^{2,5}, R. Commane⁶, B. Daube⁷, M. Dollner⁸, M. Fromm⁹, K. D. Froyd^{1,2}, A. J. Hills³, R. S. Hornbrook³, J. L. Jimenez^{2,5}, A. Kupc^{1,2,8}, K. D. Lamb^{1,2,†}, K. McKain¹⁰, F. Moore^{2,10}, D. M. Murphy¹, B. A. Nault^{2,5,11}, J. Peischl^{1,2}, A. E. Perring¹², D. A. Peterson¹³, E. A. Ray^{1,2}, K. H. Rosenlof¹, T. Ryerson^{1,§}, G. P. Schill^{1,2}, J. C. Schroder^{2,5,14}, B. Weinzierl⁷, C. Thompson^{1,2}, C. J. Williamson^{1,2¶}, S. C. Wofsy⁷, P. Yu¹⁵, J. P. Schwarz^{1*}

Pyrocumulonimbus (pyroCb) are wildfire-generated convective clouds that can inject smoke directly into the stratosphere. PyroCb have been tracked for years, yet their apparent rarity and episodic nature lead to highly uncertain climate impacts. In situ measurements of pyroCb smoke reveal its distinctive and exceptionally stable aerosol properties and define the long-term influence of pyroCb activity on the stratospheric aerosol budget. Analysis of 13 years of airborne observations shows that pyroCb are responsible for 10 to 25% of the black carbon and organic aerosols in the “present-day” lower stratosphere, with similar impacts in both the North and South Hemispheres. These results suggest that, should pyroCb increase in frequency and/or magnitude in future climates, they could generate dominant trends in stratospheric aerosol.

Pyrocumulonimbus (pyroCb) clouds, which are triggered by intense wildfires, have the potential to efficiently transport large quantities of smoke into the upper troposphere and lower stratosphere (UT/LS) (1–3). The largest of these events rival moderate volcanic eruptions in their disruption of the global radiative balance (4, 5). However, the temporal (especially long-term) and geographical extent to which these rare events affect the atmosphere are poorly known, and thus their impacts on climate and stratospheric aerosol and chemistry (including the ozone

layer) remain highly uncertain (6–8). Climate change has increased the occurrence of extreme wildfires (9–11), and pyroCb events are therefore expected to also increase in frequency in the coming decades (12, 13). To date, critical in situ measurements of pyroCb injections remain extremely limited (14–22) owing to the highly episodic nature of pyroCb and the logistical difficulties of fielding extensive airborne scientific instrument payloads on short notice. In situ measurements provide the specifics of pyroCb smoke composition (gas and aerosol phase) as well as aerosol microphysical properties that are necessary to understand the full impacts of pyroCb activity on the stratosphere.

Major pyroCb events that inject huge amounts of smoke into the stratosphere are rare; prior to 2017, only a handful of pyroCb had been observed to have perturbed the atmosphere over hemispheric spatial scales. In 2017, the largest pyroCb event observed to date in the satellite era formed in the Pacific Northwest of North America [dubbed the Pacific Northwest Event, or PNE (4)]. The ensuing smoke plume, which girdled the northern polar LS region within weeks of injection (4, 5), is estimated to have generated 0.9 K per day additional heating in the Arctic UT/LS for a month (20). The PNE smoke injection was so large that it was monitored for more than 8 months with remote-sensing techniques (21, 23) and dominated contributions to the LS from several additional pyroCb events that occurred across the Northern Hemisphere (NH) during that particularly active year of pyroCb. However, as we find here, the influence of the pyroCb smoke plume in the LS lasts over much longer time scales than merely their intense initial periods, and in-

deed longer than is possible to track with mote measurements.

Here we present detailed composition and aerosol microphysical information obtained from direct observations of pyroCb smoke in 2017. Findings drawn from their analysis are assessed in the context of in situ LS observations dating back to 2006 and are used to quantify the smoke’s average impact on LS composition. The NASA Atmospheric Tomography (ATom) mission (24), using the world’s largest atmospheric research aircraft fully outfitted with state-of-the-art instrumentation (measuring gases, particles, and meteorology), intercepted 2017 pyroCb smoke from the Pacific Northwest in the arctic LS. The aircraft conducted a series of repeated global-scale measurements that allowed direct LS sampling of the affected region approximately a year before, the year of, and the year after the injections, without intentionally targeting any air masses (Fig. 1, left). We have used these observations to advance knowledge about (i) the chemical and physical properties of pyroCb smoke, (ii) the rates of transformation of these properties, (iii) the utility of aerosol microphysical measurements to detect and track pyroCb in the LS, and (iv) the extent that pyroCb activity contributes to average LS aerosol loadings.

The first extended sampling of the 2017 smoke occurred between 7 and 11 weeks after the initial pyroCb injection. Data from this initial sampling was used to assess the chemical and physical properties of pyroCb smoke, which are needed for modeling of pyroCb plumes, their climate impacts, and their potential chemical impacts on the stratosphere. Seven months passed before a second set of observations in the same region were obtained. We used these latter measurements, in conjunction with the earlier results, to constrain the rates of transformation of key properties of the smoke aerosols, and we discovered exceptionally stable features of pyroCb smoke that can be used to “fingerprint” a fraction of pyroCb-sourced particles in the LS. No other dataset tracks pyroCb smoke over such a long period of time. Finally, using these fingerprints, we expanded consideration of stratospheric pyroCb influences to a total of 12 airborne mission datasets going back to 2006 in both the North and South Hemispheres to estimate long-term pyroCb influences on the LS in our recent climate. We found that, considering their size and frequency relative to typical fires, pyroCb are responsible for a disproportionate amount of stratospheric aerosol. These sequential findings are presented below.

The chemical composition and physical properties of stratospheric pyroCb smoke

On the first sampling of the 2017 pyroCb smoke from the tropopause up to an altitude of 12.5 km

¹National Oceanic and Atmospheric Administration (NOAA) Chemical Sciences Laboratory (CSL), Boulder, CO, USA.

²Cooperative Institute for Research in Environmental Sciences, University of Colorado, Boulder, CO, USA. ³Atmospheric Chemistry Observations and Modeling Laboratory, National Center for Atmospheric Research, Boulder, CO, USA. ⁴NASA Ames Research Center, Moffett Field, CA, USA. ⁵Department of Chemistry, University of Colorado, Boulder, CO, USA.

⁶Department of Earth and Environmental Sciences and School of Engineering and Applied Sciences, Lamont-Doherty Earth Observatory, Columbia University, Palisades, NY, USA.

⁷Department of Earth and Planetary Sciences, Harvard University, Cambridge, MA, USA. ⁸Aerosol Physics and Environmental Physics, Faculty of Physics, University of Vienna, Vienna, Austria. ⁹Naval Research Laboratory, Washington, DC, USA. ¹⁰NOAA Global Monitoring Laboratory, Boulder, CO, USA. ¹¹Center for Aerosol and Cloud Chemistry, Aerodyne Research Inc., Billerica, MA, USA. ¹²Department of Chemistry, Colgate University, Hamilton, NY, USA. ¹³Naval Research Laboratory, Monterey, CA, USA. ¹⁴Colorado Department of Public Health and Environment, Denver, CO, USA. ¹⁵Institute of Environmental and Climate Research, Jinan University, Guangzhou, People’s Republic of China.

*Corresponding author. Email: joshua.p.schwarz@noaa.gov

†Present address: Ball Aerospace, Boulder, CO, USA.

‡Present address: Department of Earth and Environmental Engineering, Columbia University, New York, NY, USA.

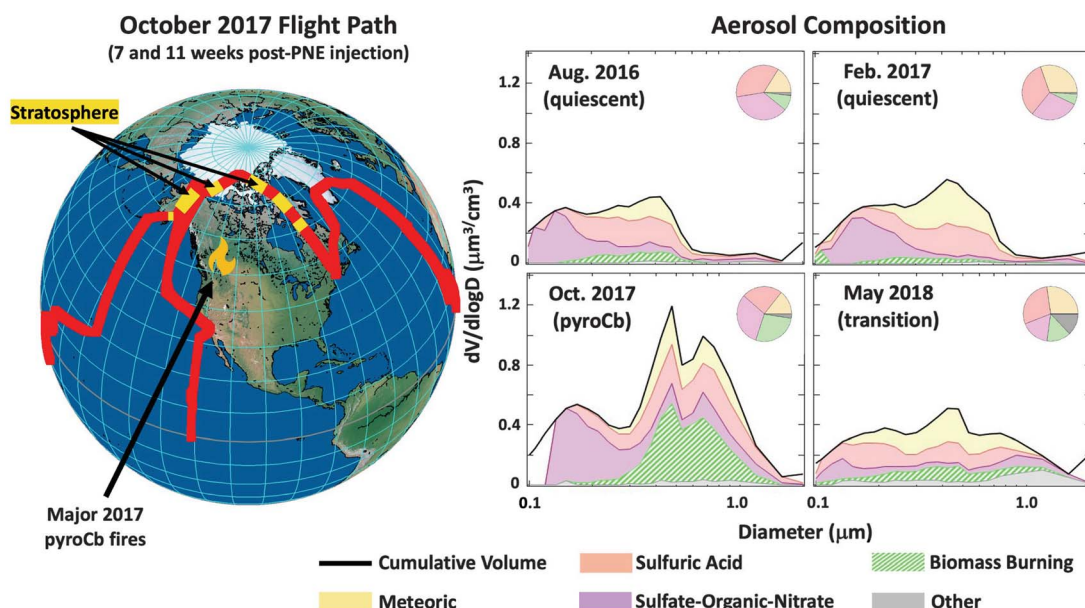
§Present address: Scientific Aviation, Boulder, CO, USA.

¶Present address: Atmospheric Composition Research, Climate Research Programme, Finnish Meteorological Institute, Helsinki, Finland.

#Present address: Institute for Atmospheric and Earth System Research, Department of Physics, Faculty of Science, University of Helsinki, Helsinki, Finland.

Downloaded from https://www.science.org at National Oceanic and Atmospheric Administration Headquarters (MAIN) on August 02, 2023

Fig. 1. Overview of in situ PNE Sampling. (Left) Relevant portions of the October 2017 flight path in the troposphere (red) and stratosphere in this paper (yellow) with British Columbia indicated by a flame symbol. (Right) Size-resolved aerosol particle-type in the Northern Hemisphere LS between August 2016 and May 2018 for particles between 0.1 and 1.5 μm (inset pie charts provide fractional comparison over all sizes). Aerosol sources from biomass burning (green) are significantly enhanced October 2017, particularly between 0.3 and 1 μm , compared with quiescent times. Note that the particle typing does not indicate mixing state.



in the stratosphere north of 55°N , concentration enhancements relative to stratospheric backgrounds were high (summarized with uncertainties in table S1). Refractory black carbon (rBC), an efficiently light-absorbing and thus climate-active species that is uniquely associated with combustion, was enhanced by a factor of 3.5, whereas organic aerosol (OA), another by-product of combustion (among other sources), was enhanced by a factor of three. Other aerosol-phase materials such as nitrate and ammonium also increased, but not by enough to allow calculation of meaningful enhancement factors. Sulfate aerosol was not enhanced in the pyroCb smoke.

Unlike the aerosol-phase materials, gas-phase biomass burning (BB) tracers [including carbon monoxide (CO), acetonitrile (CH_3CN), and others] could not be differentiated from background values in the air. When gas-phase species are scaled to the absolute rBC enhancement (~ 10 parts per thousand by mass) and their respective expected BB emissions factors (25, 26), it is clear that the related gas-phase enhancements were small relative to background variability, and in most cases on the order of instrument limits of detection. Further, the lifetimes of gaseous species such as CO and ethane (C_2H_6) in the LS are much shorter than that of rBC. Therefore, the chemical impacts of the gas-phase species from pyroCb can be expected to lose significance more quickly than those associated with aerosol-phase materials that remain distinct from backgrounds over longer times and/or at higher dilution.

The enhanced concentrations of the various species reflect the amount of injected material and its subsequent dilution at the points of sampling. However, the relative con-

centration of different species is of greater fundamental importance. Specifically, the concentration ratio of rBC to light-scattering aerosol (predominantly OA in BB smoke) is a critical parameter for relating pyroCb plume light absorption to remote measurements (23) and is needed for modeling plume radiative impacts and self-lofting. This ratio is not directly available from remote-sensing techniques. The rBC/OA ratio specific to the 2017 pyroCb sampling was determined after subtraction of typical LS concentrations for those species (details in supplementary materials). For this earliest 2017 pyroCb interception, which provides the first in situ determination of the rBC/OA ratio for a global-scale pyroCb event, the ratio was constrained to an upper bound of 0.016 ± 0.008 . This is consistent with the value (0.02) that Yu *et al.* (23) inferred from remote-sensing observations of plume loft for the PNE. We observed very similar ratios in stratospheric quiescent conditions (~ 0.016) and in fresh, non-pyroCb processed emissions from a major 2019 Washington, USA, fire (the Williams Flats Fire) that was extensively sampled (ratios of 0.012 to 0.019). It is notable that these ratios, measured over such a wide range of altitude, temperature, and age, reveal no large-scale changes in rBC/OA attributable to secondary chemistry, aerosol microphysical mechanisms, or unrelated sources and sinks large enough to drive stratospheric aerosol loads. The estimates from pyroCb measured in different ways and different stages (young, aged, diffuse, etc.) indicate the potential for reasonable uniformity in this ratio for pyroCb emissions ejected from their convective cells.

The microphysical properties of aerosols, including their size and the ways that mix-

tures of different species are found within individual particles (i.e., internally mixed), are critical to determining aerosol physical and chemical behavior and are directly quantifiable with in situ sampling. PyroCb-sourced particles have a specific feature that differs from that found both in most background LS aerosols and those associated with typical non-pyroCb wildfire emissions: PyroCb aerosols are larger than the typical accumulation mode size (yet still predominantly in the fine mode) (fig. S2). Figure 1, right, presents the very strong aerosol-volume enhancement observed in the October 2017 sampling that is solely due to BB-sourced particles in the 0.3- to 1.0- μm -diameter size range. This is larger than the bulk enhancement noted above; in this size range, BB aerosol concentration was enhanced by a factor of four over the quiescent LS conditions. Individual-particle composition measurements showed that pyroCb aerosol was predominantly organic in nature, as expected from BB (Fig. 1). This reflects the tropospheric origin of these particles and contrasts sharply with the composition expected were the aerosol material slowly formed in the stratosphere by the oxidation of sulfur-containing gases into aerosol sulfate. Further, compositional measurements of individual LS meteoric-sulfuric acid particles observed in the same air masses as the pyroCb smoke exhibited little or no organic material—a strong indication that secondary aerosol formation by the organic gases associated with the fire emissions, for example, by condensation or photochemistry, was also not strongly active in the smoke-influenced air over the time scale since injection.

We find that the most sensitive tool for collecting mixing-state information relevant to

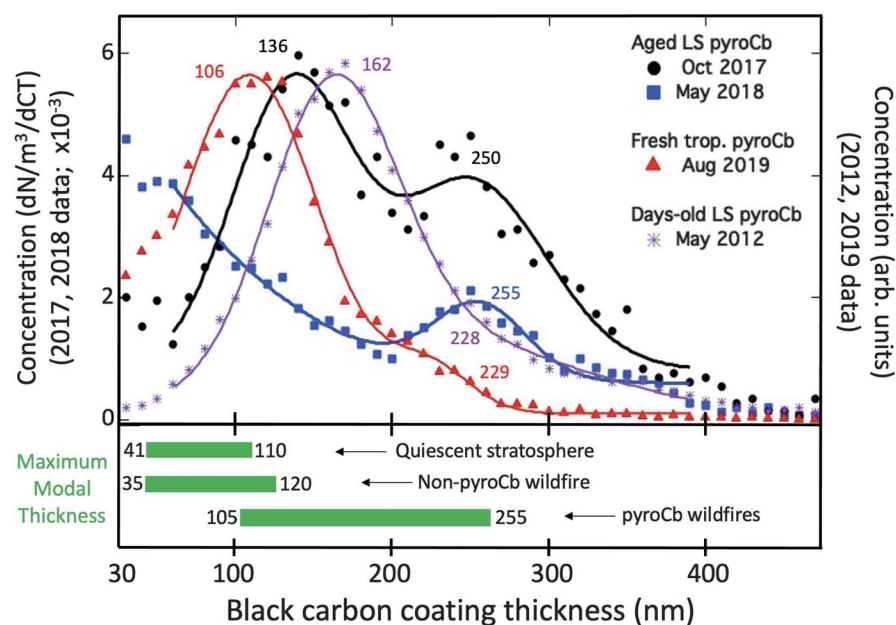


Fig. 2. The microphysical fingerprint of pyroCb. (Top) PyroCb-influenced stratospheric rBC coating thicknesses observed in October 2017 (black) and May 2018 (blue), alongside rBC coatings from fresh pyroCb smoke in the troposphere (red) and days-old LS pyroCb smoke (purple). Individual points represent in situ data; solid curves are double-Gaussian fits to those data. Inset numbers indicate the modes of the corresponding color-matched double-Gaussian curve. (Bottom) CTs in quiescent stratosphere, tropospheric wildfires, and UT/LS pyroCb smoke. Green bands represent the range of modes of observed CTs.

pyroCb activity is specific to rBC-containing particles. The large size of bulk aerosol from pyroCb translates to much larger amounts of additional aerosol material (within individual particles) associated with rBC than has been reported in past literature (18, 19, 26–29). We present this information through a quantity that scales with the amount of additional material associated with rBC: a coating thickness (CT) quantified by interpreting measured optical sizes of individual particles with consideration of their rBC mass content in a convenient (Mie shell-and-core) theoretical framework (26, 30). Figure 2 includes a histogram of CT for the LS sampling of the global-scale pyroCb smoke measured in October 2017 (black circles). The largest mode of the 2017 sampling, at ~250 nm, is larger than modes previously observed in typical (“quiescent”) stratospheric measurements (26), or direct samplings of fresh non-pyroCb wildfires plumes (27–29), where modes top out at 110 and 120 nm, respectively. Further, the tail of CT in the 2017 sampling extends beyond 400 nm, far larger than CTs reported in past observations. Larger CTs are associated with increased light absorption by rBC; here, the 250-nm-thick coating of the largest mode of the pyroCb-rBC causes ~40% more light absorption than the most thickly coated mode from non-pyroCb wildfires (at ~100-nm thickness). Averaged over the entire distribution of rBC coating thicknesses, this value is reduced to 15% higher efficiency

in absorbing light. Hence, these microphysical properties of rBC-containing aerosol, quite distinct from those produced by other sources, have complex implications for pyroCb radiative and physical impacts in the atmosphere and on climate in general.

Constraining the rates of chemical and physical transformations in stratospheric pyroCb smoke

The second sampling of the pyroCb smoke that originated in 2017 occurred 7 months after the first, after remote-sensing techniques could no longer clearly detect the smoke in the sampled airmasses. However, these measurements did not occur in otherwise unperturbed conditions. Rather, a separate influence of large-scale dust and pollution transport also contributed to bulk enhancements of aerosol. Hence, the bulk composition and chemical makeup of the aerosol could not be meaningfully used to track changes specifically in the pyroCb-sourced material. However, although the bulk enhancement of rBC changed (and may have also been influenced by the additional input to the air), the rBC-specific microphysical characteristics of the pyroCb-aerosol remained distinct.

Figure 2 shows that the most heavily coated rBC mode (blue squares) was present with virtually unchanged size, meaning that no appreciable further accumulation or degradation of the internally mixed material had occurred. The consistency between this mode observed

in October 2017 and May 2018 is notable. Considering that just a small fraction, roughly 2%, of aerosol particles that we sampled in the stratosphere during October 2017 were found to contain rBC, at first look this finding does not appear to be relevant to the bulk of the pyroCb smoke. However, because the material internally mixed with the rBC can reasonably be expected to act as a chemical proxy for the bulk aerosol from pyroCb, the implications of this finding are broad. The stability of the measured CT points to the chemical and physical stability of all pyroCb smoke in the LS. This finding, that the pyroCb smoke properties are so stable in the LS, coupled with the consistently smaller range of CT from non-pyroCb wildfires, hints that strong convective lifting is the dominant mechanism determining the properties of the smoke injected into the LS via pyroCb activity. We speculate that a combination of aqueous and/or ice phase processes and coagulation and enhanced condensation of low-volatility gases within the convective column of the pyroCb drive fast transformations of aerosol to the near-stable state existing after injection into the LS. The formation of heavily coated rBC appears to be a general accumulation-mode aerosol characteristic of pyroCb smoke in the stratosphere. Interestingly, the 2017 distribution is consistent with the aerosol size distribution from a known pyroCb smoke plume interception that occurred in 2002 (15, 25), which also presents an atypically large total-aerosol particle distribution (fig. S2).

Our observation of the exceptional long-term physical stability of pyroCb-sourced aerosol in the LS contradicts contemporary expectations that UT/LS OAs undergo destructive photochemical reactions on timelines of 5 months and could imply wider and longer-term impacts from pyroCb (and potentially biomass burning more generally) in this region than previously anticipated. Specifically, Yu *et al.* (23) achieved a 150-day model lifetime for pyroCb organics in the LS by modeling photochemical destruction to match decay in remote-sensing observations, and a 250-day lifetime in the absence of such chemistry (via transport and/or dilution). Tropospheric studies by Hodzic *et al.* (31) and Lou *et al.* (32) inferred from tropospheric simulations that relatively strong chemical or photolytic removal was needed to reproduce UT secondary organic aerosols. Those lifetimes imply changes in rBC coating thickness of 30 and 20% over 7 months, respectively, inconsistent with the observed stability demonstrated by the ~250-nm CT mode measured in 2017 and 2018. Rather, our observations are consistent with older conclusions from in situ measurements (33) that carbonaceous particles larger than 300 nm can persist in the stratosphere for many months without undergoing mass depletion. If chemistry only negligibly destroys pyroCb aerosol in the LS,

then the main sinks in this region will be limited to those associated with large-scale transport and stratospheric-tropospheric exchange and sedimentation mechanisms. If this is also true for the upper troposphere, then previous studies may have incorrectly ascribed other loss processes such as wet deposition to photochemical loss. The lifetimes obtained from remote measurements of high-altitude plumes may instead reflect dilution and mixing into the larger stratosphere. In fact, our estimate of the e -folding time for such mixing, derived from the observed concentration change of the large-coating rBC mode, is ~ 5 months, consistent with the observations on the dissolution of the larger pyroCb plume at higher altitudes (23).

Fingerprints of pyroCb persist in LS aerosol microphysical properties

The distinctive and persistent aerosol microphysical features introduced above remained discernible in the LS longer than any other feature of the injection measured either remotely or by in situ techniques. In fact, because of both their persistence and the contrast they provide to rBC emitted by non-pyroCb sources, we find that measurements of thickly coated rBC concentrations can be used to assess the long-term influence of pyroCb activity in the LS. First we explore the contrast, then we test its utility for identifying pyroCb aerosol contributions in LS data obtained since 2006. Figure 2 shows that pyroCb events can generate larger coating thickness modes (modes up to 255 nm) than non-pyroCb fires (modes up to 120 nm). Further, we find a contrast in the percentage of rBC-containing particles with CTs greater than 200 nm ($P_{>200}$) from different sources. In both the published literature (26–29) and an expansive set of previously unpublished open-burning smoke data (African smoke encountered during the NASA ATom and North American wildfires sampled during the 2019 NASA/NOAA FIREX-AQ mission), we find that non-pyroCb BB sources generate $P_{>200}$ on average of just 2% with a standard deviation of 1%. PyroCbs generate $P_{>200}$ at least as high as 37% (tables S2 and S3). Two unpublished pyroCb CT distributions shown in Fig. 1 provide further support for the occurrence of these pyroCb smoke characteristics over a wider altitude range. On 14 May 2012, days-old smoke transported through the stratosphere from a pyroCb event in Russia was sampled at 12 km over the continental US. The rBC within that plume was heavily coated (Fig. 1, purple curve), with a primary mode at 162 nm, a secondary mode at 228 nm, and a tail extending beyond 300 nm. More recently, we obtained direct sampling of a small-scale pyroCb in the troposphere at 8- to 9-km altitude within hours of emission from the August 2019 Williams Flats Fire in Washington,

USA (34). CTs from that dataset (Fig. 2, red triangles) again exhibit heavily coated rBC populations enhanced over those of a typical wildfire with a secondary CT mode centered at 229 nm. The CT distributions from both these events showed $P_{>200}$ well beyond 3%.

Examination of two published UT/LS pyroCb smoke samplings using the same rBC-measurement technique used here provide additional case studies fully consistent with our findings. Dahlkötter *et al.* (18) sampled days-old pyroCb smoke in the UT/LS and reported evidence for a CT mode at 160 nm, with a shoulder extending at least to 250 nm. Ditas *et al.* (19) sampled wildfire smoke in the LS and reported large CTs with the tail of the distribution extending beyond 300 nm. We have revisited the back-trajectory analysis of that sampling (fig. S4) and now associate it unequivocally with a pyroCb event in Siberia (details in supplementary materials). Although individual modes are less evident in that dataset than here, Ditas *et al.* inferred large CT modes by decomposing the distribution into multiple Gaussians; their pyroCb-affected coating thickness distribution shows a mode at ~ 220 nm. These publications did not include $P_{>200}$ values. Note that we also observed stratospheric air with low $P_{>200}$. These observations rule out the possibility of widespread generation of CTs larger than 200 nm by interactions of convective columns with non-pyroCb smoke; such an effect would be expected to provide a much more regular signal on a seasonal basis. In total, we are not aware of any noteworthy nonlaboratory sources of rBC that produce coatings in the larger pyroCb range (fossil fuel sources generate $P_{>200} \sim 0$). Our observations and the associated literature search indicate that $P_{>200}$ of $>2\%$ are unequivocally produced by pyroCb, that only pyroCb generate CT modes of >120 nm, and large non-pyroCb sources typically only generate $P_{>200}$ of $\leq 3\%$.

To test the utility of these features, we identified evidence of convincing pyroCb influence in an extensive collection of airborne campaigns spanning the past 13 years, limited to data in the LS over a wide latitude range (table S4). We examined these large datasets of stratospheric air for observations of CT distributions with at least one mode at thicknesses larger than those seen from non-pyroCb wildfires (i.e., >120 nm), while simultaneously having $P_{>200}$ of five standard deviations above that of non-pyroCb sources (table S3). The published literature provides information on independently documented pyroCb activity.

Most of the datasets did not indicate strong pyroCb influence, consistent with a lack of known pyroCb activity affecting their sampled regions or time windows. However, clear instances of pyroCb influence were indeed found (“flagged”). The earliest example of

obvious pyroCb contributions being flagged occurred in the LS at roughly 30°N latitude in July 2007 (TC4 mission; see supplementary materials). In this case, the influence was traced back to the Milford Flat pyroCb in Utah, USA, which occurred 1 week prior. The CT distribution is bimodal, with the larger mode at 169 nm. Southern Hemisphere LS air was flagged in March 2010 during research flights south of New Zealand (HIPPO mission; see supplementary materials). We attribute this to a February 2010 pyroCb formation in western Australia, from which long-range transport of aerosol layers were clearly visible at ~ 12 km by remote sensing (35). Earlier sampling in this region, in 2009, was also flagged, with a clear CT mode at 179 nm and $P_{>200} \sim 27\%$. A case can be made to link the flagging to the major Australian Black Saturday fires ~ 9 months prior, although satellite imagery indicated that LS conditions were consistent with quiescent periods by June 2009 (36). On the basis of our findings here, that the CT signatures of 2017 injections were the longest-lived discernible features of the pyroCb smoke in the LS, and that ~ 10 months after injection we observed $P_{>200} \sim 22\%$, this association is reasonable. Finally, a flagging occurred at about the same time in the NH, with $P_{>200} \sim 12\%$. We do not find an associated documented pyroCb event but consider this case a good illustration of the value of these measurements used for identifying potential pyroCb injections in the LS, especially in the historical record prior to the recent proliferation in pyroCb research.

Constraining pyroCb influence in the lower stratosphere

The long-term persistence of thickly coated rBC in the LS, together with the associations we found between such features and documented pyroCb events, supports the use of this microphysical fingerprint to infer pyroCb influence in the LS even when it is not generating a five-standard deviation enhancement in $P_{>200}$, as above. In this case, the fractional contributions of pyroCb to the entire LS rBC population are estimated on the basis of observed $P_{>200}$ coupled with assumptions about different source characteristic and some simple algebra (tables S3 to S5 and supplementary text). In brief, we assume different fixed-source values for $P_{>200}$ produced by pyroCb and non-pyroCb (i.e., all other rBC sources) and calculate the relative contributions of each on the basis of the observed number fraction. Having attributed the rBC sourced by pyroCb in this way, we have a powerful proxy for all the pyroCb-sourced aerosol in the air mass. This attribution provides no information on LS aerosols arising from different sources (e.g., mineral dust, sulfate, etc.).

Our reexamination of the 13 years of in situ stratospheric data collected in both the Northern and Southern Hemispheres has produced statistically significant estimates of long-term pyroCb influence in each hemisphere. These are the first such estimates based on in situ sampling of pyroCb smoke in the stratosphere and are not obtainable from remote-sensing or other bulk-aerosol techniques. These data were assembled from both localized (i.e., collected with research aircraft operating from a fixed base) and global-scale campaigns (i.e., with aircraft transiting across wide latitude ranges from near one pole to the other). None of the campaigns targeted pyroCb influence, so all the sampling was unbiased. Each set of measurements typically extended over ~1 month. We have 12 independent measurements for the NH and 9 for the Southern Hemisphere (SH). For much of these data (all the SH data and >80% of the NH data), concurrent sulfur hexafluoride (SF₆) concentration measurements were available and were evaluated. SF₆, a long-lived tracer of anthropogenic origin, follows the large-scale movement of air in the stratosphere as driven by the Brewer-Dobson circulation, with entry of rising air in the tropics that then arches over a range of altitudes to descend at the poles. Depending on the path taken by a particular air parcel, its age after entry into the stratosphere can vary widely before finally reaching the poles, with faster transport occurring at lower altitudes (see supplementary materials for the surface trends, observed SF₆ histograms, and mean age of air related to altitude in the LS). SF₆ measurements enabled analysis of pyroCb as a function of mean age of air or mean altitude in the stratosphere and provide context to how representative our findings are in the LS.

We find that pyroCb activity has an impact on stratospheric rBC much larger than expected given their relative frequency and size compared with non-pyroCb fires and other sources of rBC. Over the entire 13-year dataset, pyroCb activity increased rBC in the NH LS by 10 to 25%, and by 10 to 22% in the SH LS. These ranges reflect uncertainties arising from the assumptions on source-dependent microphysical characteristics for rBC, statistical uncertainty, and variations depending on inclusion or exclusion of the strong pyroCb late-2017 NH observations in the calculations. This attribution for rBC can be approximately associated with OA on the basis of the reasonable stability of rBC/OA ratios explored above in fresh wildfire plumes, UT/LS pyroCb smoke, and in the quiescent LS (supplementary materials). On average, these results were obtained for air of 1-year mean age in the NH, and 1.5 years in the SH. Analysis of the subset of LS air that spent on average 3 years since surface interactions (corresponding to a range

of 5 to 10 km above the tropopause in the stratosphere) produces a very similar pyroCb influence estimate with poorer statistics. This strengthens the relevance of these attribution fractions to larger volumes of stratospheric air, over longer times. The supplementary materials include a mass-balance check based on the measurements made 10 months after the PNE, when the smoke can be assumed to be well mixed in the background, and show that these results are not unphysical.

Implications

PyroCb efficiently inject aerosols with distinctive features into the UT/LS, and those aerosols survive without significant photochemical or chemical degradation for time scales of at least 1 year and make up ~1/5 of all lower stratospheric rBC and OA over decadal time scales.

The aerosol fingerprints of pyroCb can be used to detect pyroCb compositional contributions over a wide range of magnitudes and air mass age in the LS, even as their local concentrations decrease to levels below the detection threshold of remote-sensing or in situ gas-phase measurements, and without any need for a priori knowledge of specific pyroCb events. Using them to constrain pyroCb influence in the LS informs mechanisms of stratospheric dynamics and chemistry from other potentially important perturbations of the LS. These include volcanoes, rocket emissions, climate interventions, nuclear winter, and supersonic transport emissions. Hence these findings are very broadly relevant.

The direct transport of pyroCb aerosols to the stratosphere explains the heightened influence of pyroCb activity on the region compared with typical wildfires. For example, the PNE represents only a small fraction of the 2017 NH burned area and only ~5% of the CO emissions (37, 38). Yet nearly 1 year later, it was still responsible for ~40% of the black carbon aerosol well mixed into the NH LS and observed in untargeted sampling (table S5). This result was so unexpected that we performed a simple mass balance test to confirm that it is physical. Clearly, representation of large pyroCb events in models is necessary to capture both year-to-year stratospheric variability at this level and shorter-term larger radiative impacts. The radiative effects of the PNE were recently estimated through modeling (39) to manifest a net negative top of the atmosphere forcing. This result was strongly dependent on rapid atmospheric adjustments in the stratosphere driven by localized heating by the smoke. By extension, the long-term pyroCb influence found here would also provide a net-negative influence, approximately one-fifth that of the typical LS.

Although the fractional importance of pyroCb activity to total LS aerosol varies with the

strength of non-pyroCb sources to this background (for example, oxidation of sulfur species to sulfate), it is such an efficient transport pathway of aerosol that it may well have a dominant impact on either future trends of stratospheric aerosol or their uncertainties. This speculation springs from expectations for increases in both atmospheric instability and wildfire frequency, size, and geographic distribution, which could have strong synergistic impacts on pyroCb frequency and strength (12, 13, 40, 41). Indeed, some of these expectations are already being met: The pyroCb “super” outbreak in Australia during 2019 and 2020 injected three times more smoke into the stratosphere than the PNE (42). Clearly, the significance of pyroCb activity to stratospheric aerosol highlights the importance of robust predictions of pyroCb development, frequency, and size both currently and in future climates, because these events have tremendous potential to shift global stratospheric aerosol composition and chemistry, as well as dynamics (7, 8, 39).

REFERENCES AND NOTES

1. M. Fromm et al., *Geophys. Res. Lett.* **27**, 1407–1410 (2000).
2. M. D. Fromm, R. Servranckx, *Geophys. Res. Lett.* **30**, 1542 (2003).
3. M. Fromm et al., *Bull. Am. Meteorol. Soc.* **91**, 1193–1210 (2010).
4. D. A. Peterson et al., *NPJ Clim. Atmos. Sci.* **1**, 30 (2018).
5. S. M. Khaykin et al., *Geophys. Res. Lett.* **45**, 1639–1646 (2018).
6. D. A. Peterson et al., *J. Appl. Meteorol. Climatol.* **56**, 471–493 (2017).
7. S. Solomon et al., *Proc. Natl. Acad. Sci. U.S.A.* **119**, e2117325119 (2022).
8. P. Bernath, C. Boone, J. Crouse, *Science* **375**, 1292–1295 (2022).
9. E. S. Kasischke, M. R. Turetsky, *Geophys. Res. Lett.* **33**, L09703 (2006).
10. J. T. Abatzoglou, A. P. Williams, *Proc. Natl. Acad. Sci. U.S.A.* **113**, 11770–11775 (2016).
11. A. L. Westerling, *Philos. Trans. R. Soc. London Ser. B* **371**, 20150178 (2016).
12. D. A. Peterson, E. J. Hyer, J. R. Campbell, J. E. Solbrig, M. D. Fromm, *Mon. Weather Rev.* **145**, 2235–2255 (2017).
13. G. Di Virgilio et al., *Geophys. Res. Lett.* **46**, 8517–8526 (2019).
14. A. E. Waibel et al., *Chemosphere, Glob. Chang. Sci.* **1**, 233–248 (1999).
15. H. J. Jost et al., *Geophys. Res. Lett.* **31**, 1–5 (2004).
16. P. K. Hudson et al., *J. Geophys. Res.* **109**, D23S27 (2004).
17. E. A. Ray, *J. Geophys. Res.* **109**, D18304 (2004).
18. F. Dahlkötter et al., *Atmos. Chem. Phys.* **14**, 6111–6137 (2014).
19. J. Ditas et al., *Proc. Natl. Acad. Sci. U.S.A.* **115**, E11595–E11603 (2018).
20. K. Christian et al., *Geophys. Res. Lett.* **46**, 10061–10071 (2019).
21. O. Torres et al., *J. Geophys. Res. Atmos.* **125**, e2020JD032579 (2020).
22. J. J. D. Hooghiem et al., *Atmos. Chem. Phys.* **20**, 13985–14003 (2020).
23. P. Yu et al., *Science* **365**, 587–590 (2019).
24. C. R. Thompson et al., *Bull. Am. Meteorol. Soc.* **103**, E761–E790 (2022).
25. M. Fromm, D. Peterson, L. Di Girolamo, *J. Geophys. Res. Atmos.* **124**, 13254–13272 (2019).
26. J. P. Schwarz et al., *J. Geophys. Res.* **113**, D03203 (2008).
27. J. W. Taylor et al., *Atmos. Chem. Phys.* **14**, 13755–13771 (2014).
28. A. E. Perrin et al., *J. Geophys. Res. Atmos.* **122**, 1086–1097 (2017).

29. J. Ko, T. Krasowsky, G. Ban-Weiss, . *Atmos. Chem. Phys.* **20**, 15635–15664 (2020).
30. J. P. Schwarz *et al.*, *Geophys. Res. Lett.* **35**, L13810 (2008).
31. A. Hodzic *et al.*, *Atmos. Chem. Phys.* **16**, 7917–7941 (2016).
32. S. Lou *et al.*, *J. Adv. Model. Earth Syst.* **12**, e2020MS002266 (2020).
33. D. M. Murphy, D. J. Cziczo, P. K. Hudson, D. S. Thomson, *J. Geophys. Res.* **112**, D04203 (2007).
34. D. A. Peterson *et al.*, *Bull. Am. Meteorol. Soc.* **103**, E2140–E2167 (2022).
35. A. Foth *et al.*, *Atmos. Chem. Phys.* **19**, 6217–6233 (2019).
36. J. M. Siddaway, S. V. Petelina, *J. Geophys. Res.* **116**, D06203 (2011).
37. H. C. Pumphrey *et al.*, *Atmos. Chem. Phys.* **21**, 16645–16659 (2021).
38. C. Wiedinmyer *et al.*, *Geosci. Model Dev.* **4**, 625–641 (2011).
39. C. C. Liu *et al.*, *Geophys. Res. Lett.* **49**, (2022).
40. J. Chen, A. Dai, Y. Zhang, K. L. Rasmussen, *J. Clim.* **33**, 2025–2050 (2020).
41. M. Taszarek, J. T. Allen, M. Marchio, H. E. Brooks, *NPJ Clim. Atmos. Sci.* **4**, 35 (2021).
42. D. A. Peterson *et al.*, *NPJ Clim. Atmos. Sci.* **4**, 38 (2021).
43. S. C. Wofsy *et al.*, ATom: Merged Atmospheric Chemistry, Trace Gases, and Aerosols, version 2, ORNL DAAC (2021); <https://doi.org/10.3334/ORNLDAAC/1925>.

ACKNOWLEDGMENTS

We thank the ATom science team and leadership, the DC-8 pilots and crew for their outstanding commitment to the mission, and K. Aikin of NOAA CSL for assistance with creating the figures. **Funding:** This work was supported by the ATom investigation under NASA's Earth Venture program (grant NNX15AJ23G). Elements of the manuscript were supported by the National Center for Atmospheric Research, which is a major facility sponsored by the National Science Foundation under cooperative agreement 1852977. A.K. was supported by the Austrian Science Fund's Erwin Schrodinger Fellowship J-3613. B.A.N., J.C.S., P.C.-J., and J.L.J. were supported by NASA grants NNX15AH33A and 80NSSC21K1451. D.A.P. was supported by the Naval Research Laboratory Base Program and NASA Modeling, Analysis, and Prediction (MAP) Program (80HQTR21T0099). J.M.K., I.B., P.C.-J., K.D.F., J.L.J., A.K., K.D.L., K.M., F.M., B.A.N., J.P., E.A.R., G.P.S., J.C.S., C.T., and C.J.W. were fully or partly supported by NOAA cooperative agreement NA17OAR4320101. B.W. and M.D. have received funding from the European Research Council (ERC) under the European Union's Horizon 2020 research and innovation program under grant agreement 640458 (A-LIFE). Additional support was provided by the University of Vienna. **Author contributions:** Data collection and curation: E.C.A., A.E.P., F.M., I.B., C.A.B., K.M., T.P.B., P.C.-J., R.C., B.D., M.D., K.D.F., A.J.H., R.S.H., J.L.J., A.K., K.D.L., D.M.M., B.A.N., J.P., E.A.R., T.R., G.P.S., J.C.S., B.W., C.T., C.J.W., S.C.W., and J.P.S. Analysis: E.C.A., I.B., C.A.B., T.P.B., P.C.-J., R.C., B.D., M.D., K.D.F., A.J.H., R.S.H., J.L.J., A.K., D.M.M., B.A.N., J.P., T.R., G.P.S.,

J.C.S., B.W., C.T., C.J.W., S.C.W., and J.P.S. Funding acquisition: S.C.W., T.R., and J.P.S. Methodology: J.M.K., P.C.-J., M.F., K.D.F., J.L.J., D.M.M., D.A.P., G.P.S., P.Y., and J.P.S. Writing, review, and editing: All authors. **Competing interests:** The authors declare that they have no competing interests. **Data and materials availability:** rBC microphysical property data from past field campaigns and ATom used here are available at <https://csl.noaa.gov/groups/csl6/measurements/data/2022-Katich-et-al/>. All other data are from ATom and have been deposited with the Oak Ridge National Laboratory Distributed Active Archive Center (ORNL DAAC) (43). **License information:** Copyright © 2023 the authors, some rights reserved; exclusive licensee American Association for the Advancement of Science. No claim to original US government works. <https://www.science.org/about/science-licenses-journal-article-reuse>

SUPPLEMENTARY MATERIALS

science.org/doi/10.1126/science.add3101
 Materials and Methods
 Supplementary Text
 Figs. S1 to S5
 Tables S1 to S4
 References (44–54)

Submitted 3 June 2022; accepted 31 January 2023
 10.1126/science.add3101



Pyrocumulonimbus affect average stratospheric aerosol composition

J. M. Katich, E. C. Apel, I. Bourgeois, C. A. Brock, T. P. Bui, P. Campuzano-Jost, R. Commane, B. Daube, M. Dollner, M. Fromm, K. D. Froyd, A. J. Hills, R. S. Hornbrook, J. L. Jimenez, A. Kupc, K. D. Lamb, K. McKain, F. Moore, D. M. Murphy, B. A. Nault, J. Peischl, A. E. Perring, D. A. Peterson, E. A. Ray, K. H. Rosenlof, T. Ryerson, G. P. Schill, J. C. Schroder, B. Weinzierl, C. Thompson, C. J. Williamson, S. C. Wofsy, P. Yu, and J. P. Schwarz

Science, **379** (6634), .

DOI: 10.1126/science.add3101

Fired up

Large wildfires can generate pyrocumulonimbus clouds that transport smoke into the stratosphere and have major impacts on the stratospheric aerosol budget and climate. Katich *et al.* analyzed 13 years of airborne observations to determine the chemical and physical compositions of pyrocumulonimbus smoke and to quantify its effects on stratospheric aerosols. These clouds are responsible for as much as 25% of the black carbon and organic aerosols now in the lower stratosphere and may become an even more important influence on future climate as the frequency and severity of extreme fires increase. —HJS

View the article online

<https://www.science.org/doi/10.1126/science.add3101>

Permissions

<https://www.science.org/help/reprints-and-permissions>

Use of this article is subject to the [Terms of service](#)

Science (ISSN) is published by the American Association for the Advancement of Science. 1200 New York Avenue NW, Washington, DC 20005. The title *Science* is a registered trademark of AAAS.

Copyright © 2023 The Authors, some rights reserved; exclusive licensee American Association for the Advancement of Science. No claim to original U.S. Government Works